

A computational method for the Hufnagel pseudocylindric map projection family

Bernhard Jenny^{a,b}, Bojan Šavrič^{a,c} and Daniel R. Strebe^d

^aCollege of Earth, Ocean, and Atmospheric Sciences, Oregon State University, Corvallis, OR, USA; ^bSchool of Science, RMIT University, Melbourne, Australia; ^cEsri Inc., Redlands, CA, USA; ^dMaphematics LLC, Seattle, WA, USA

ABSTRACT

In 1989, Herbert Hufnagel introduced a mathematical model for a family of equal-area, pseudocylindric projections, which includes the Mollweide, Wagner IV, and Eckert IV projections as specializations. Hufnagel's contribution has received very little attention, and his projections are not available in any of the commonly used cartographic software packages. This article makes three contributions: The Hufnagel family is introduced to the English-speaking community; algorithms for computing the forward and reverse projections are presented; and the eight new projections proposed by Hufnagel are analyzed.

ARTICLE HISTORY

Received 2 July 2015
Accepted 24 November 2015

KEYWORDS

Hufnagel; Mollweide; Eckert IV; Wagner IV; world map projection; small-scale projection

Introduction: the Hufnagel projection family

In 1989, in the German-language journal *Kartographische Nachrichten*, Herbert Hufnagel introduced a generalization of the Mollweide projection that includes the Eckert IV and Wagner IV projections and other useful equal-area pseudocylindric world map projections (Hufnagel 1989). In the same article, he also proposed eight new equal-area pseudocylindric projections. The method by Hufnagel, who was a professor at the Fachhochschule München (now Munich University of Applied Sciences), allows for the creation of a variety of equal-area pseudocylindric projections that are useful for practical map making. Additionally, smooth transitions between projections can be computed, which can be useful for animated or user-controlled transformations between projections. Hufnagel's projections are not currently available in any cartographic software package.

The only reference to the Hufnagel projection family that we could identify in the literature is by Čapek (2001), who compared various world map projections. While Čapek found that the distortion of Hufnagel's projections compares favorably to other commonly used world map projections, he did not, however, develop code for the projection equations. Instead, he based his evaluation of the projections on a graphical analysis of the graticules included in Hufnagel's (1989)

publication (personal communication with R. Čapek, April and May 2014).

Cartographers are not unanimous as to what projections are best used for world maps. Besides distortion characteristics, the appearance and aesthetic preference are important factors when selecting a world map projection (Jenny, Patterson, and Hurni 2008). For example, Šavrič et al. (2015) found that map readers prefer pseudocylindric map projections (with straight parallels) to world map projections with curved parallels. Hufnagel's equal-area projections are pseudocylindric, and cartographers can tune their appearance to their aesthetical preference by adjusting a set of projection parameters.

Hufnagel's projection family includes the Mollweide, Eckert IV, Wagner IV, and any cylindrical equal-area projection. By adjusting projection parameters, a variety of intermediate projections can be created, and when projection parameters continuously change over time, smooth transitions between these projections can be created. There is potential for Hufnagel's equal-area transformation method to be applied in modified form to other projections. It could possibly be added to the adaptive composite map projection technique by Jenny (2012), which adjusts the map projection to the geographical area displayed by the map. We therefore believe that the details of Hufnagel's method and projections merit to be documented and presented to the

English-speaking community. It is our hope that with this contribution, Hufnagel's projections will be included in cartographic software packages, and the methods involved will help further the field and provide more to build upon.

The following section introduces Hufnagel's method; the description is loosely based on Hufnagel (1989). The next section provides equations and an algorithm using a look-up table for the conversion of spherical coordinates to Cartesian planar coordinates. This algorithmic method is also useful for fast implementations of the Mollweide, Eckert IV, and other projections. The last section documents the eight pseudocylindrical equal-area projections introduced by Hufnagel. Appendix 1 proves that the cylindrical projection is a limiting case of the Hufnagel projection.

Hufnagel's development

Hufnagel (1989) started with the Mollweide projection using a polar coordinate system. An ellipse for the antimeridian (which forms the map boundary) is constructed by applying an affine stretching to a circle, which results in varying the distance of the antimeridian from the central meridian (see Figure 1). The affine transformation, however, is not achieved by applying different scale factors to x - and y -coordinates, but the distance r from the projection's origin is modulated with cosine curves with double and quadruple periods, using amplitude factors A and B . Equation (1) expresses this general development (Hufnagel 1989). The graticule is constructed by mirroring the first quadrant along the x - and y -axes (Figure 1). The resulting map boundary is symmetric relative to the x -axis (the equator) and the y -axis (the central meridian) for any A and B , and they intersect both axes at right angles. With $A = 0$ and $B = 0$, a circle is obtained with radius $r = 1$ (Figure 1).

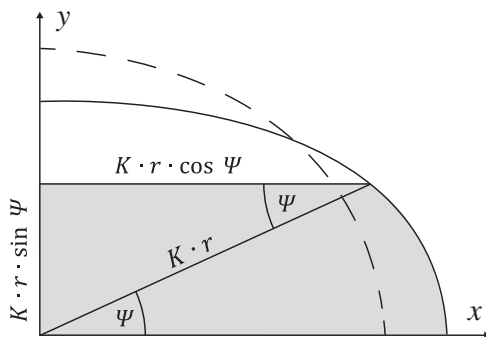


Figure 1. The affine stretching by modulating the radius r with cosine curves (after Hufnagel 1989).

$$\begin{aligned}x_{\pi} &= K \cdot r \cdot \cos \Psi \\y &= K \cdot r \cdot \sin \Psi \\r^2 &= 1 + A \cdot \cos 2\Psi + B \cdot \cos 4\Psi\end{aligned}\quad (1)$$

In Equation (1), x_{π} and y are the projected coordinates of the map boundary, Ψ is a parametric angle (the angle from the positive direction of the x -axis to a point on the map boundary), r is the distance from the origin to a point on the map boundary, A and B are amplitudes defining r , and K is a scale factor.

By changing the parameters A and B , a variety of projections can be created. With the selection of an appropriate mathematical relationship between the parametric angle Ψ and the geographic latitude φ , equal-area projections can be developed. The equal-area property is maintained when the sum of area highlighted in gray in Figure 1 is equal to half of the area between the equator and latitude φ (which is $\pi \cdot \sin \varphi$). From this condition one can derive the relation shown in Equation (2). Equation (3) is identical to Equation (2), but Hufnagel eliminates r^2 using Equation (1) (Hufnagel 1989). In Equations (2) and (3), φ is the geographic latitude; Ψ , r , A , B , and K are defined as above.

$$\begin{aligned}\pi \cdot \sin \varphi &= \frac{K^2}{2} \int_0^{\Psi} r^2 d\Psi + \frac{K^2}{2} r^2 \cdot \sin \Psi \cdot \cos \Psi \\&= \frac{K^2}{4} \left(2 \int_0^{\Psi} r^2 d\Psi + r^2 \sin 2\Psi \right) \\&= \frac{K^2}{4} \left(2\Psi + A \cdot \sin 2\Psi + \frac{B}{2} \sin 4\Psi + r^2 \cdot \sin 2\Psi \right),\end{aligned}\quad (2)$$

$$\begin{aligned}\pi \cdot \sin \varphi &= \frac{K^2}{4} \left(2\Psi + \left(1 + A - \frac{B}{2} \right) \sin 2\Psi \right. \\&\quad \left. + \frac{A+B}{2} \sin 4\Psi + \frac{B}{2} \sin 6\Psi \right).\end{aligned}\quad (3)$$

When $\varphi = 90^\circ$, the corresponding Ψ in Equation (3) is the maximum parametric angle Ψ_{\max} . For $\Psi_{\max} = 90^\circ$, poles are represented with points. When Ψ_{\max} is smaller than 90° , projections have pole lines. Appendix 1 proves that when Ψ_{\max} approaches 0, the Hufnagel projection transforms into an equal-area cylindrical projection.

The value of the constant K in Equations (1)–(3) can be obtained from Equation (3) by setting $\varphi = 90^\circ$, $\Psi = \Psi_{\max}$, and using the selected amplitudes A and B (see also Equation (7)). To project the longitude λ , the x -coordinate of the antimeridian is multiplied by λ/π (Equation (4)) (Hufnagel 1989).

$$x = \frac{\lambda}{\pi} \cdot x_{\pi} = K \cdot \frac{\lambda}{\pi} \cdot r \cdot \cos \Psi \quad (4)$$

The final step in Hufnagel's derivation is an equal-area stretching applied to the projected x - and y -coordinates. The stretching factor C adjusts the map to the equator-to-central meridian ratio desired by the cartographer (Equation (5)). The factor C is computed with Equation (6), where α is the equator-to-central meridian ratio, and Ψ_{\max} is the maximum parametric angle. K is computed from A , B , and Ψ_{\max} with Equation (7).

$$x = \frac{K \cdot C}{\pi} \cdot \lambda \cdot r \cdot \cos \Psi, y = \frac{K}{C} \cdot r \cdot \sin \Psi \quad (5)$$

$$C^2 = \alpha \cdot \sin \Psi_{\max} \cdot \sqrt{\frac{1 + A \cdot \cos 2\Psi_{\max} + B \cdot \cos 4\Psi_{\max}}{1 + A + B}} \quad (6)$$

Using Hufnagel's derivation approach, the Mollweide projection is created by first setting the amplitude factors A and B to 0, which results in a circular map boundary. Then, the equal-area condition is applied to the circle using Equation (3) to compute a parametric angle Ψ for each latitude φ . The maximum parametric angle Ψ_{\max} is set to 90° , because the Mollweide projection represents poles as points. And finally, equal-area stretching with the factor $C = \sqrt{2}$ (Equation (6)) is applied to set the equator-to-central meridian ratio α to 2. Computational techniques are detailed in the next section.

Tobler's hyperelliptical projection family also includes the Mollweide projection (Tobler 1973). However, Tobler and Hufnagel's projection families are parameterized differently and have considerably different characteristics. Tobler uses a family of curves called the hyperellipse, while Hufnagel uses a family of curves that has no particular name. Unlike Tobler's hyperellipses, Hufnagel's curves have inflection points, which results in a greater diversity in his projection family. As a practical matter for computation, Hufnagel's development also does not require numerical integration.

Some aspects of Hufnagel's derivation are similar to Wagner's area-preserving transformation method called *Umbeziffern*, meaning renumbering (Wagner 1931, 1932, 1941, 1949, 1962). With the parametric angle Ψ , new latitude values are computed, and the

map is adjusted to the preferred equator-to-central meridian ratio with the stretching factor C .

Algorithms for Hufnagel's projection family

Individual members of Hufnagel's projection family are created by configuring four parameters: $A \in [-1, 1]$, $B \in [-1, 1]$, $\Psi_{\max} \in [0, \frac{\pi}{2}]$, and C , which is a stretching factor that adjusts the map to the preferred equator-to-central meridian ratio. This section details algorithmic steps for applying the parameters.

Direct equations for transforming spherical coordinates to planar Cartesian coordinates do not exist for Hufnagel's projection family. To compute a parametric angle Ψ for a corresponding latitude φ with Equation (3), an iteration procedure has to be used. This is a well-known characteristic of the Mollweide projection (Mollweide 1805; Snyder 1987, 1993) and the Eckert IV projection (Eckert 1906; Snyder 1987, 1993). Using the Newton-Raphson method, the iteration process to find Ψ for a given latitude φ is as follows:

- (1) Selection of a seed value Ψ_0 for the unknown parametric angle Ψ .
- (2) Correction $\Delta\Psi$ with Equation (8).
- (3) Improved value of the parametric angle: $\Psi_{n+1} = \Psi_n - \Delta\Psi$

The calculation is repeated until $|\Delta\Psi| < \varepsilon$ (a small threshold value). The selection of a seed value for the parametric angle in step 1 is critical for the iterative procedure to converge. We found no heuristic for a seed value that works across all parameterizations of the projection. Therefore, we built three lookup tables, each with the same size (we used 101 elements each). The first table contains linearly increasing values of the parametric angle $\Psi \in [0, \Psi_{\max}]$. It serves as an "index" into the other two tables, one of which goes forward to the y value computed from Ψ , and the other of which goes backward to the φ value computed from the same Ψ . The tables represent the relationship between Ψ , y , and φ given fixed A , B , C , and Ψ_{\max} . For a given Ψ appearing in the first table, the corresponding y value and φ value appear at the same index in their own respective tables. We index off of Ψ rather than off of φ

$$K^2 = \frac{4\pi}{2 \cdot \Psi_{\max} + (1 + A - \frac{B}{2}) \cdot \sin 2\Psi_{\max} + \frac{A+B}{2} \cdot \sin 4\Psi_{\max} + \frac{B}{2} \cdot \sin 6\Psi_{\max}} \quad (7)$$

$$\Delta\Psi = \frac{\frac{K^2}{4} (2 \cdot \Psi_n + (1 + A - \frac{B}{2}) \cdot \sin 2\Psi_n + \frac{A+B}{2} \cdot \sin 4\Psi_n + \frac{B}{2} \cdot \sin 6\Psi_n) - \pi \sin \varphi}{\frac{K^2}{2} (1 + (1 + A - \frac{B}{2}) \cdot \cos 2\Psi_n + (A + B) \cdot \cos 4\Psi_n + \frac{3B}{2} \cdot \cos 6\Psi_n)} \quad (8)$$

or y in order to avoid having to iterate when calculating the tables, since y and φ both can be calculated in closed form from Ψ . Algorithm 1 presents pseudocode for the initialization of the lookup tables (with the number of elements equal to $TableSize$).

Algorithm 1. Initialization of the lookup tables

```

1: for  $i \in [0, TableSize - 1]$  do
2:    $\Psi = \frac{i \cdot \Psi_{\max}}{TableSize - 1}$ 
3:   if  $i = 0$  then
4:      $\varphi = 0$ 
5:   else if  $i = (TableSize - 1)$  then
6:      $\varphi = 90^\circ$ 
7:   else
8:      $\varphi$  from Equation (3)
9:   end if
10:   $r$  from Equation (1)
11:   $y$  from Equation (5)
12:  if  $i > 0$  then
13:    if  $y < yTable[i - 1]$  or  $\varphi < latitudeTable[i - 1]$  then
14:      raise folding graticule exception
15:    end if
16:  end if
17:   $paramAngleTable[i] = \Psi$ 
18:   $latitudeTable[i] = \varphi$ 
19:   $yTable[i] = y$ 
20: end for

```

Algorithm 1 uses the lookup table for the y -coordinate to identify combinations of the parameters A , B , and Ψ_{\max} that result in y values failing to increase monotonically with φ , in which case an exception is raised (lines 13–15). In other words, $\delta y / \delta \varphi$ goes negative, causing some higher latitudes to end up closer to the equator on the map than lower latitudes do. This could be detected more analytically but was not deemed worth the effort; given the size of the look-up tables, only a tiny uncertainty remains in detecting failure of monotonicity while also yielding robust seed values.

To select a robust seed value for the parametric angle Ψ for a latitude φ , we first find the two closest latitudes in the latitude lookup table using a binary search. The seed value for the parametric angle Ψ is found with linear interpolation between the corresponding parametric angles extracted from the lookup table. With this approach, the seed value of Ψ is very close to the exact value. Algorithm 2 presents pseudocode for the selection of a seed value Ψ_0 of the parametric angle Ψ from the lookup tables.

Algorithm 2. Finding seed value Ψ_0 of the parametric angle Ψ

Input: φ

```

1:  $i_{\min} = 0$ 
2:  $i_{\max} = TableSize$ 
3: repeat
4:    $i_{mid} = \lfloor \frac{i_{\max} + i_{\min}}{2} \rfloor$ 
5:   if  $i_{mid}$  equals  $i_{\min}$  then
6:     break loop
7:   else if  $|\varphi| > latitudeTable[i_{mid}]$  then
8:      $i_{\min} = i_{mid}$ 
9:   else
10:     $i_{\max} = i_{mid}$ 
11:   end if
12: end loop
13:  $\varphi_1 = latitudeTable[i_{\min}]$ 
14:  $\varphi_2 = latitudeTable[i_{\min} + 1]$ 
15:  $weight = \frac{|\varphi - \varphi_1|}{\varphi_2 - \varphi_1}$ 
16:  $\Psi_1 = paramAngleTable[i_{\min}]$ 
17:  $\Psi_2 = paramAngleTable[i_{\min} + 1]$ 
18:  $\Psi_0 = weight \cdot (\Psi_2 - \Psi_1) + \Psi_1$ 
19: return  $\varphi < 0 ? -\Psi_0 : \Psi_0$ 

```

After calculating the parametric angle Ψ , the Cartesian coordinates are obtained with Equation (5). Algorithm 3 presents pseudocode for the computation of Cartesian coordinates from spherical coordinates.

Algorithm 3. Projecting spherical coordinates to Cartesian coordinates

Inputs: λ and φ

```

1: Find seed value  $\Psi_0$ . (Algorithm 2)
2: repeat
3:    $\Delta \Psi_{\text{numerator}}$  of Equation (8)
4:   if  $|\Delta \Psi_{\text{numerator}}| < \epsilon$ 
5:     break loop
6:   end if
7:    $\Delta \Psi_{\text{denominator}}$  of Equation (8)
8:    $\Delta \Psi = \frac{\Psi_{\text{numerator}}}{\Delta \Psi_{\text{denominator}}}$ 
9:    $\Psi_{n+1} = \Psi_n - \Delta \Psi$ 
10: end loop
11:  $r$  with Equation (1)
12:  $x$  with Equation (5)
13:  $y$  with Equation (5)
14: return  $[x, y]$ 

```

The Mollweide, Eckert IV, and Wagner IV projections have direct reverse equations. However, general members of the Hufnagel projection family require an iteration procedure. The Newton–Raphson method can be used with Equation (9) to find the correction $\Delta\Psi$ of the parametric angle for a given y -coordinate (r is defined in Equation (1)).

For the selection of a seed value Ψ_0 , the parametric angle and y -coordinate look-up tables are used. The algorithm used to find the seed value is similar to Algorithm 2, except the y -coordinate is used instead of the latitude value. After the parametric angle Ψ is computed, the latitude can be obtained from Equation (3) and the longitude is computed from Equation (5). Algorithm 4 shows pseudocode for determining spherical coordinates from Cartesian coordinates.

Algorithm 4. Projecting Cartesian coordinates to spherical coordinates

Inputs: x and y

- 1: Find seed value Ψ_0 . (Algorithm 2, using y -coordinate lookup table)
 - 2: **repeat**
 - 3: $\Delta\Psi_{\text{numerator}}$ of Equation (9)
 - 4: **if** $|\Delta\Psi_{\text{numerator}}| < \varepsilon$
 - 5: break loop
 - 6: **end if**
 - 7: $\Delta\Psi_{\text{denominator}}$ of Equation (9)
 - 8: $\Delta\Psi = \frac{\Psi_{\text{numerator}}}{\Delta\Psi_{\text{denominator}}}$
 - 9: $\Psi_{n+1} = \Psi_n - \Delta\Psi$
 - 10: **end loop**
 - 11: r with Equation (1)
 - 12: φ with Equation (3)
 - 13: λ with Equation (5)
 - 14: **return** $[\lambda, \varphi]$
-

Hufnagel's eight projections

Hufnagel introduced eight new projections for world maps, which are all members of his map projection family (Hufnagel 1989). The eight projections are named Hufnagel II, III, IV, VII, IX, X, XI, and XII. The numbering is not continuous, as Hufnagel did not

use the numerals I, V, VI, and VIII. Those respective positions are occupied by the Mollweide, Wagner IV (Snyder 1993; Wagner 1949, 1962), Eckert IV projections, and an approximation of the Eckert VI projection (Hufnagel 1989). Figure 2 illustrates the projections proposed by Hufnagel, and Table 1 details the parameters A , B , and Ψ_{max} , and the equator-to-central meridian ratio α (which is defined as a function of the stretching factor C ; see Equation (5)).

All projections in Figure 2 have an equator-to-central meridian ratio of 2:1, except for the Hufnagel XII projection, which has a ratio of 2.44. The Mollweide and the Hufnagel II, III and IV projections show the poles as points. Hufnagel (1989) noted that his II, III, and IV projections have less overall distortion than the Mollweide projection. This can be confirmed by the weighted mean error in the overall scale distortion indices and the mean angular deformation indices (Canters and Declair 1989), as well as by Čapek's acceptance index (Čapek 2001). Results are shown in Table 2. Figure 3 shows local distortion patterns for the 12 projections by means of lines of constant maximum angular deformation.

The eight projections in the second and third columns in Figure 2 show the pole points as lines. The length of the pole lines of the Eckert IV, Wagner IV, and Hufnagel VII, VIII, and X projections is half the equator length. The length of the pole line of the Hufnagel IX projection is slightly shorter. Meridians of the Wagner IV, the approximated Eckert VI, and the Hufnagel VII projections meet the pole lines with an obtuse angle. The ends of the meridians of the Eckert IV and the Hufnagel IX and X projections are tangent with the pole lines, that is, they smoothly transition into the pole lines. The distortion indices of these projections are very similar (Table 2). Hufnagel comments that in his opinion, number IX is the most aesthetically balanced projection (Hufnagel 1989).

The Hufnagel XI projects the poles as points, but meridional convergence is so rapid toward the poles that the poles can look like lines. Due to the unusual boundary of this projection, Hufnagel states that its visual appearance is debatable (Hufnagel 1989).

The Hufnagel XII projection has pole lines that have almost the same length as the equator. Meridians slightly bend where they approach the pole line, resulting in a projection that loosely resembles cylindrical equal-area projections. The Hufnagel XII projection

$$\Delta\Psi = \frac{r^2 \cdot \sin^2\Psi_n - \left(\frac{y \cdot C}{K}\right)^2}{\sin 2\Psi_n \cdot (1 - A + 2B + (2A - 4B) \cdot \cos 2\Psi_n + 3B \cdot \cos 4\Psi_n)} \quad (9)$$

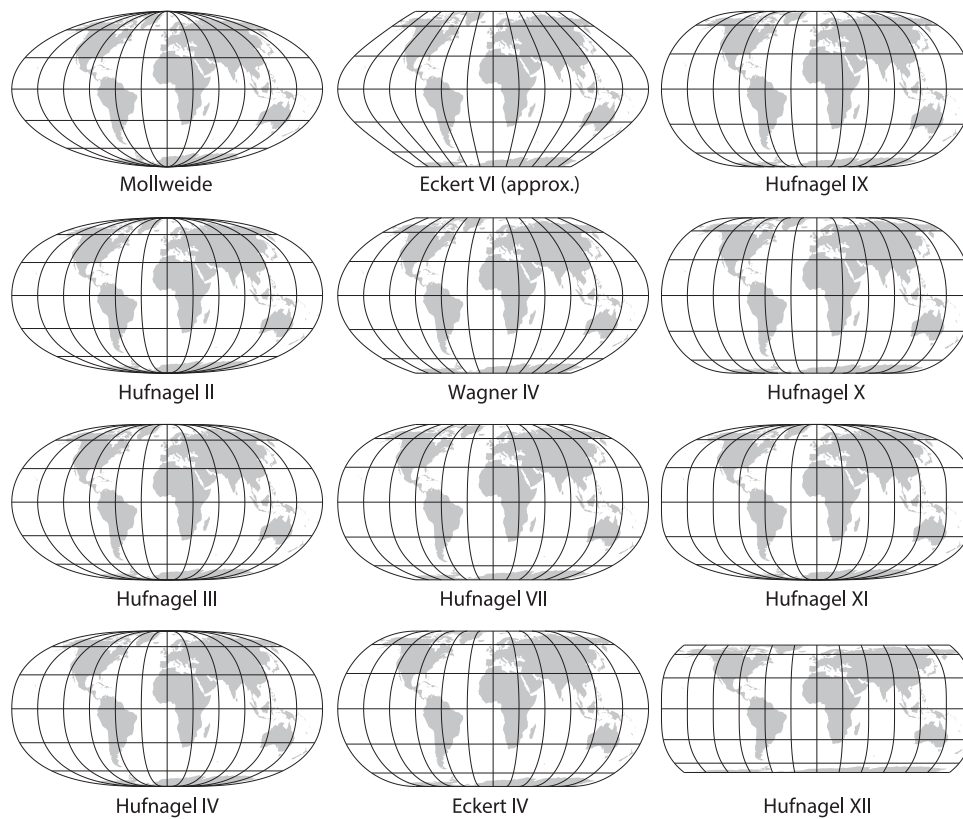


Figure 2. The 12 projections presented by Hufnagel (1989) ordered by columns (Hufnagel did not use the numerals I, V, VI, VIII; the Mollweide, Wagner IV, Eckert IV and an approximation of the Eckert VI projection occupy the corresponding positions).

Table 1. The 12 projections presented by Hufnagel (1989) with their parameters.

Projection	A	B	Ψ_{\max}	α
Mollweide	0	0	90	2
Hufnagel II	1/18	-1/18	90	2
Hufnagel III	0.5	1/18	90	2
Hufnagel IV	1/12	-1/12	90	2
Eckert VI (approx.)	-2/21	2/21	60	2
Wagner IV	0	0	60	2
Hufnagel VII	1/12	-1/12	60	2
Eckert IV	1	0	45	2
Hufnagel IX	2/3	1/3	45	2
Hufnagel X	-2/3	2/3	30	2
Hufnagel XI	0	-1/9	90	2
Hufnagel XII	0	-1/9	40	2.44

has the smallest mean angular deformation index of the 12 projections (Table 2).

Conclusion

Hufnagel proposes an interesting family of map projections that includes the Mollweide, Eckert IV, and Wagner IV projections as special cases. Additional projections can be created by varying the parameters A , B , and Ψ_{\max} , and the equator-to-central meridian ratio of the map. Hufnagel's method is very flexible and allows for creating a variety of equal-area pseudocylindrical projections. Many

Table 2. Distortion indices for the projections presented by Hufnagel (1989): the weighted mean error in the overall scale distortion index D_{ab} (Canters and Declair 1989), the mean angular deformation index D_{an} (Canters and Declair 1989), and the area percentage with acceptable areal and angular distortion Q (Čapek 2001).

Projection	D_{ab}	D_{an}	Q
Mollweide	0.39	32.28	70.6
Hufnagel II	0.37	30.33	75.8
Hufnagel III	0.37	30.27	76.7
Hufnagel IV	0.36	29.52	77.8
Eckert VI (approx.)	0.40	32.43	69.5
Wagner IV	0.38	30.39	76.3
Hufnagel VII	0.36	28.97	79.7
Eckert IV	0.36	28.73	81.9
Hufnagel IX	0.36	28.80	81.6
Hufnagel X	0.36	28.22	83.2
Hufnagel XI	0.36	28.81	78.3
Hufnagel XII	0.42	25.79	79.7

parameter combinations result in absurd distortion characteristics or folding graticules that are of little value for practical map making (Figure 4). We explored valid ranges of the A , B , and Ψ_{\max} parameters that result in non-folded graticules, but the distribution pattern of valid combinations is very irregular and difficult to visualize. Many projections in this pseudocylindrical projection family have nevertheless reasonable distortion properties, and seem to be useful for a variety of equal-area world

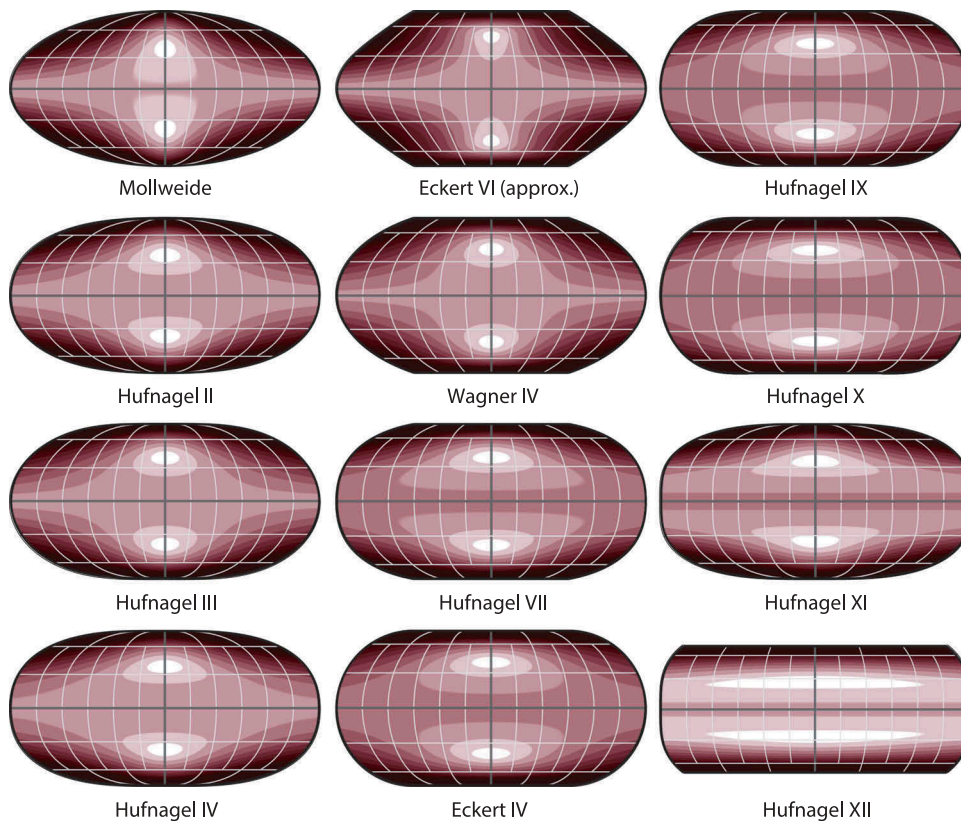


Figure 3. Lines of constant maximum angular deformation for the 12 projections, 6° increments.

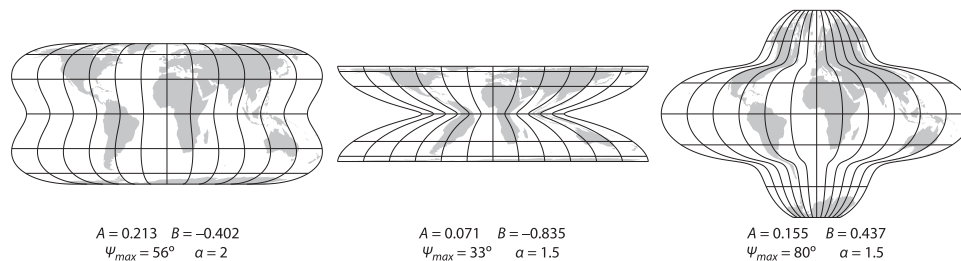


Figure 4. Outlandish projections illustrating the flexibility of Hufnagel's method.

maps. We recommend using a specialized graphical user interface coupled with a WYSIWYG map visualization for selecting projection parameters when creating a customized Hufnagel projection (an example for the Hufnagel projection family is available at <https://www.mapmathematics.com/interactive/hufnagel.html>).

The Hufnagel projections will be available in the next version of the *Geocart* software (<https://www.mapmathematics.com>). The computational method and algorithms presented in this article were implemented in the open-source Java Map Projection Library (<https://github.com/OSUCartography/JMapProjLib>). We hope that this contribution will help Hufnagel's projection family find its place in other cartographic

projection libraries and software applications, and eventually on world maps.

Acknowledgements

The authors would like to thank Richard Čapek, Tomas Bayer (Charles University, Prague), Jan D. Bláha (Jan Evangelista Purkyně University, Ústí nad Labem, Czechia), and Rolf Böhm (Ingenieurbüro für Kartographie, Bad Schandau, Germany) for their help and comments. The support of Esri, Inc. is greatly acknowledged. We also thank Abby Metzger and Gareth Baldrice-Franklin, Oregon State University, for editing this text and figures, and the anonymous reviewers for their valuable comments.

Disclosure statement

No potential conflict of interest was reported by the authors.

References

- Canter, F., and H. Declair. 1989. *The World in Perspective: A Directory of World Map Projections*. Chichester, UK: John Wiley and Sons.
- Čapek, R. 2001. "Which Is the Best Projection for the World Map?" Paper presented at the 20th International Cartographic Conference, Beijing, China, August 6–10. http://icaci.org/files/documents/ICC_proceedings/ICC2001/icc2001/file/f24014.pdf
- Eckert, M. 1906. "Neue Entwürfe für Erdkarten." *Petermanns Mitteilungen* 52 (5): 97–109.
- Hufnagel, H. 1989. "Ein System unecht-zylindrischer Kartennetze für Erdkarten." *Kartographische Nachrichten* 39 (3): 89–96.
- Jenny, B. 2012. "Adaptive Composite Map Projections." *IEEE Transactions on Visualization and Computer Graphics* 18 (12): 2575–2582. <http://dx.doi.org/10.1109/TVCG.2012.192>
- Jenny, B., T. Patterson, and L. Hurni. 2008. "Flex Projector—Interactive Software for Designing World Map Projections." *Cartographic Perspectives* 59: 12–27. doi:10.14714/CP59.245.
- Mollweide, K. B. 1805. "Über die vom Prof. Schmidt in Giessen in der zweyten Abtheilung seines Handbuchs der Naturlehre S. 595 angegebene Projection der Halbkugelfläche." *Zach's monatliche Correspondenz zur Beförderung der Erd- Und Himmels-Kunde* 8: 152–163.
- Šavrič, B., B. Jenny, D. White, and D. R. Strebe. 2015. "User Preferences for World Map Projections." *Cartography and Geographic Information Science* 42 (5): 398–409. doi:10.1080/15230406.2015.1014425.
- Snyder, J. P. 1987. *Map Projections: A Working Manual*. Geological Survey Professional Paper 1395. US Government Printing Office: Washington, DC, 383 pp.
- Snyder, J. P. 1993. *Flattening the Earth. Two Thousand Years of Map Projections*. Chicago: University of Chicago Press.
- Tobler, W. R. 1973. "The Hyperelliptical and Other New Pseudo Cylindrical Equal Area Map Projections." *Journal of Geophysical Research* 78 (11): 1753–1759. doi:10.1029/JB078i011p01753.
- Wagner, K. H. 1931. "Die unechten Zylinderprojektionen: Ihre Anwendung und ihre Bedeutung für die Praxis." Doctoral dissertation, Mathematisch-Naturwissenschaftliche Fakultät, University of Hamburg.
- Wagner, K. H. 1932. "Die unechten Zylinderprojektionen." *Aus dem Archiv der Deutschen Seewarte* 51 (4): 68.
- Wagner, K. H. 1941. "Neue ökumenische Netzentwürfe für die kartographische Praxis." In *Jahrbuch der Kartographie 1941*, edited by E. Lehmann, 176–202. Leipzig: Bibliographisches Institut.
- Wagner, K. H. 1949. *Kartographische Netzentwürfe*. Leipzig: Bibliographisches Institut.
- Wagner, K. H. 1962. *Kartographische Netzentwürfe*. 2nd ed. Mannheim: Bibliographisches Institut.

Appendix 1. Equal-area cylindrical projection as limiting case of the Hufnagel projection

This appendix proves that Hufnagel's projection family transforms into the equal-area cylindrical projection, when Ψ_{\max} approaches 0. An expression of φ for Hufnagel's projection is:

$$\sin \varphi = \frac{4\psi + [2 + 2A + 2A \cos(2\psi) + 2B \cos(4\psi)] \sin(2\psi) + B \sin(4\psi)}{4\psi_{\max} + [2 + 2A - B] \sin(2\psi_{\max}) + [A + B] \sin(4\psi_{\max}) + B \sin(6\psi_{\max})}.$$

Any particular value of ψ is some fraction k of ψ_{\max} , where $[0 \leq k \leq 1]$. In finding the limit as both ψ and ψ_{\max} approach 0, then, we first change the function to one variable by substituting $k \psi_{\max}$ everywhere for ψ :

$$\sin \varphi = \frac{4k\psi_{\max} + [2 + 2A + 2A \cos(2k\psi_{\max}) + 2B \cos(4k\psi_{\max})] \sin(2k\psi_{\max}) + B \sin(4k\psi_{\max})}{4\psi_{\max} + [2 + 2A - B] \sin(2\psi_{\max}) + [A + B] \sin(4\psi_{\max}) + B \sin(6\psi_{\max})}.$$

We cannot directly evaluate $\sin \varphi$ when $\psi_{\max} = 0$ because the fraction is indeterminate. L'Hôpital's Rule states:

$$\lim_{x \rightarrow c} \frac{f(x)}{g(x)} = \lim_{x \rightarrow c} \frac{f'(x)}{g'(x)}$$

Therefore to find the value of $\sin \varphi$ as $\psi_{\max} \rightarrow 0$,

$$\begin{aligned} \sin \varphi &= \lim_{\psi_{\max} \rightarrow 0} \frac{\frac{d}{d\psi_{\max}} (4k\psi_{\max} + [2 + 2A + 2A \cos(2k\psi_{\max}) + 2B \cos(4k\psi_{\max})] \sin(2k\psi_{\max}) + B \sin(4k\psi_{\max}))}{\frac{d}{d\psi_{\max}} (4\psi_{\max} + [2 + 2A - B] \sin(2\psi_{\max}) + [A + B] \sin(4\psi_{\max}) + B \sin(6\psi_{\max}))}} \\ &= \lim_{\psi_{\max} \rightarrow 0} k \left[\frac{4 - 4A + 8A \cos^2(2k\psi_{\max}) - 8B \sin(2k\psi_{\max}) \sin(4k\psi_{\max}) + 4 \cos(2k\psi_{\max}) + 4A \cos(2k\psi_{\max}) + 4B \cos(2k\psi_{\max}) \cos(4k\psi_{\max}) + 4B \cos(4k\psi_{\max})}{4 - 2B \cos(2\psi_{\max}) + 4 \cos(2\psi_{\max}) + 4A \cos(2k\psi_{\max}) + 4A \cos(4\psi_{\max}) + 4B \cos(4\psi_{\max}) + 6B \cos(6\psi_{\max})} \right] \end{aligned}$$

$$= k.$$

Now, to find the limit of x and y as $\psi_{\max} \rightarrow 0$, we express x and y as series with the same $\psi = k \psi_{\max}$ substitution, and truncating all terms that are not constant, since they evaluate to 0:

$$\begin{aligned} x &= \lambda \sqrt{\frac{a}{\pi}} \\ y &= k \sqrt{\frac{\pi}{a}} \end{aligned}$$

But as we just saw, $k = \sin \varphi$, so

$$\begin{aligned} x &= \lambda \sqrt{\frac{a}{\pi}} \\ y &= \sin \varphi \sqrt{\frac{\pi}{a}} \end{aligned}$$

in the cylindrical case, as expected.